Accepted Manuscript

Water-Based 3D Inkjet Printing of an Oral Pharmaceutical Dosage Form

Hatim K. Cader, Graham A. Rance, Morgan R. Alexander, Andrea D. Gonçalves, Clive J. Roberts, Chris J. Tuck, Ricky D. Wildman

Please cite this article as: H.K. Cader, G.A. Rance, M.R. Alexander, A.D. Gonçalves, C.J. Roberts, C.J. Tuck, R.D. Wildman, Water-Based 3D Inkjet Printing of an Oral Pharmaceutical Dosage Form, *International Journal of Pharmaceutics* (2019), doi: https://doi.org/10.1016/j.ijpharm.2019.04.026

Water-Based 3D Inkjet Printing of an Oral

Pharmaceutical Dosage Form

Hatim K. Cader [a*], Graham A. Rance [b], Morgan R. Alexander [c], Andrea D. Gonçalves [d],

Clive J. Roberts [c], Chris J. Tuck [a], Ricky D. Wildman [a]

[a] Centre for Additive Manufacturing, Faculty of Engineering, University of Nottingham, Nottingham, NG7 2RD, UK

[b] Nanoscale and Microscale Research Centre, Cripps South, University of Nottingham, University Park, Nottingham NG7 2RD, UK

[c] Advanced Materials and Healthcare Technologies, School of Pharmacy, University of Nottingham, University Park, Nottingham, NG7 2RD, UK

[d] DPDD Drug Delivery, GlaxoSmithKline R&D, Gunnels Wood Road, Stevenage, SG1 2NY, UK

* Corresponding author

Email: hatim.cader@nottingham.ac.uk

Telephone: +44(0)115 84 66374

Address : Centre for Additive Manufacturing, Faculty of Engineering, University of Nottingham, Nottingham, NG7 2RD, UK

Abstract

Inkjet printing is a form of additive manufacturing where liquid droplets are selectively deposited onto a substrate followed by solidification. The process provides significant potential advantages for producing solid oral dosage forms or tablets, including a reduction in the number of manufacturing steps as well as the ability to tailor a unique dosage regime to an individual patient. This study utilises solvent inkjet printing to print tablets through the use of a Fujifilm Dimatix printer. Using polyvinylpyrrolidone and thiamine hydrochloride (a model excipient and drug, respectively), a water-based ink formulation was developed to exhibit reliable and effective jetting properties. Tablets were printed on polyethylene terephthalate films where solvent evaporation in the ambient environment was the solidification mechanism. The tablets were shown to contain a drug loading commensurate with the composition of the

ink, in its preferred polymorphic phase of a non-stoichiometric hydrate distributed homogenously. The printed tablets displayed rapid drug release. This paper illustrates solvent inkjet printing's ability to print entire free-standing tablets without an edible substrate being part of the tablet and the use of additional printing methods. Common problems with solvent-based inkjet printing, such as the use toxic solvents, are avoided. The strategy developed here for tablet manufacturing from a suitable ink is general and provides a framework for the formulation for any drug that is soluble in water.

Keywords: Solvent inkjet printing, tablet, drug delivery, water-based, additive manufacturing

1 INTRODUCTION

Additive manufacturing (AM), commonly referred to as 3D printing, is a process where materials are built up layer-by-layer (ASTM International, 2013). Material or inkjet printing is one amongst many AM processes and is defined as a process where liquid material is selectively jetted onto a substrate (Gibson et al., 2010). The jetting process consists of three phases: 1) droplet generation, 2) positioning and interaction of ink droplets with a substrate and 3) a solidification mechanism (Derby, 2010). Inkjet printing can involve the continuous jetting of droplets (a catcher is used to collect unwanted jetted droplets) or with a drop-on-demand (DOD) mechanism (Martin et al., 2008). DOD inkjet printing can further be categorised based on the mechanism of droplet generation. In some cases, a thermal resistor is rapidly heated which causes the vapourisation of the surrounding ink. In turn, a vapour bubble is formed and grows until a droplet is forced out of the nozzle. When the heater is turned off, a transient pressure wave is generated allowing stable ink ejection (Cummins and Desmulliez, 2012). Alternatively, a piezoelectric material can be used, where a voltage is applied to the material resulting in a mechanical deformation that ejects the ink droplets. In many cases, the use of a piezoelectric material may be more advantageous than the use of a thermal resistor as some inks may be heat sensitive or degrade in response

2

to heat. The solidification mechanism can occur in different ways including solvent evaporation (He et al., 2016), UV curing (He et al., 2017) or a chemical reaction (reactive jetting) (Sturgess et al., 2017).

The main challenge for inkjet printing is the development of a reliable printable ink that can also maintain its end product functionality. A 'printability' factor, Z, has been derived that takes into account the properties of both the ink and the printer to determine how well an ink will print (Equation 1). The equation relates the surface tension (γ), viscosity (η), density (ρ) and its droplet size (a), which is determined by the nozzle diameter of the printer cartridge. Ideally, the Z-value will be between 1 and 10 for reliable and effective jetting (Derby, 2010). Its inverse value, known as the Ohnesorge (Oh) number is frequently used as a substitute. It generally accepted that surface tension should be within the range of 20 and 50 mN·m^{-1} (Hoath, 2016) and viscosity within 8 and 15 mPa·s (Magdassi, 2009), although this can vary significantly depending on the specific printer used.

$$Z = \frac{1}{Oh} = \frac{(\gamma \rho a)^{\frac{1}{2}}}{\eta} \quad (1)$$

The current production route for tablets is typically by powder compression methods (Gibson, 2009). These are well suited for mass manufacture, but have limitations in terms of personalisation of dose due to the large number of steps involved in manufacturing tablets (Zhang et al., 2004). These challenges could be addressed through AM of tablets, which has fewer steps and is able to produce personalised tablets. Through inkjet printing specifically, there are potentially only three main stages of the manufacturing of the tablet form: ink preparation, the jetting of material and the solidification mechanism. It has been showed in the past that it is a highly programmable technology that is easily customised, making it ideal for personalisation (Fox et al., 2017). The productionisation of inkjet printing is at topic that has been investigated for medical devices by Baumers et al., 2018. The authors investigate factors that impact manufacturing of heavily regulated products including the risk of build failure and develop a

3

cost model. The authors notes that the results from this research are critical to inform future work on the viability of AM for it to be adapted by any industry (Baumers et al., 2018).

Numerous AM processes have been used to manufacture drug delivery systems, including binder jetting (Wu et al., 1996), material extrusion (Khaled et al., 2015), vat photo-polymerisation (Wang et al., 2016), powder bed fusion (Fina et al., 2018) and inkjet printing (Clark et al., 2017). The different printing mechanisms and parameters can be manipulated to gain greater customisation of the device.

For inkjet printing specifically, one of the greatest advantages is the ability to control the drug release through a number of printing parameters including the size or surface area of a printed geometry (Desai et al., 2010), loading of jetted droplets (Scoutaris et al., 2011), printing on substrates that affect crystallisation (Sandler et al., 2011), varying the droplet spacing on a substrate and the freedom of spatial location of a drug in a delivery system (Genina et al., 2013). High dosing levels have been achieved to a high degree of uniformity (Scoutaris et al., 2011), reproducibility (Hirshfield et al., 2014) and accuracy for high resolution applications (Genina et al., 2013). Inkjet printing has also illustrated its potential to develop formulations for poorly soluble active pharmaceutical ingredients (APIs) through the use of nanosuspension (with a modified water-based formulation) (Pardeike et al., 2011), nanoplexes (Cheow et al., 2015) and even simple solvent systems (Wickström et al., 2015), although inkjet printing here was used as a dosing technique instead of a stand-alone manufacturing process. A photo curable ink with a hydrophilic drug has also been used to jet into preformed blank tablets (Acosta-Vélez et al., 2017). Inkjet printing has also been used to dose drugs (topotecan) and biologics (insulin) into planar micro-devices for oral delivery (Fox et al., 2017). As the inkjet system used was easily programmable (highlighting ease of potential of personalisation), experimental parameters such printing and drying cycles allowed large drug loading capacities in contrast to other techniques where the drug loading is limited due to solubility. The process did not require any UV light or heat which would not damage or degrade sensitive biologics and

4

drugs. The authors highlight the use of inkjet printing for creating low-waste but high-capacity loading devices for different drug-containing micro-devices (Fox et al., 2017).

The examples given previously always include the use of a substrate, containers or another printing process (e.g. electrospinning (Palo et al., 2017) and flexographic printing (Genina et al., 2012)) to create the dosage form. There have been detailed investigations using different imaging methods as a quality control process, with inkjet printing (e.g. hyperspectral imaging (Vakili et al., 2014), colorimetry (Wickström et al., 2016) and Raman spectroscopy (Edinger et al., 2017)). Drug containing solutions have also been printed in the pattern of quick response codes onto hypromellose material, illustrating inkjet printing's ability to create functional labelling and quality control measures (Edinger et al., 2018). The ability to wholly manufacture a tablet solely through inkjet printing has only recently been achieved (Kyobula et al., 2017).

Kyobula et al., 2017 used fenofibrate and beeswax as the drug's carrier to print tablets through hot melt jetting. The drug was mixed with the beeswax and heated in the printer and jetted in its molten form, which then solidified on the print bed. The authors showed that it was possible to make use of the high printing accuracy to create a complex honeycomb internal structure. Through varying the cell size of the printed honeycomb, the drug release profile could be controlled (Kyobula et al., 2017). Clark et al., 2017 utilised UV-curable inks for the production of tablets with a hydrophilic drug. The materials used were known from previous publications to exhibit good biocompatibility, but the authors note that any uncured monomer, macromer and photo-initiator degradation products would need to be identified. It was illustrated, however, that the process resulted in a high degree of UV curing, highlighting UV inkjet printing as a potentially acceptable process for tablet production (Clark et al., 2017). Acosta-Vélez et al., 2018 created a photo-curable bioink for hydrophobic drugs. The authors jetted poly(ethylene glycol) diacrylate (250 Da), with Eosin Y as a biocompatible photo initiator and methoxide-poly(ethylene glycol)-amine as a co-initiator allowing for free radical polymerisation. Naproxen was used as the API

5

and poly(ethylene glycol) (200 Da) as a plasticiser. Controlled release was achieved by varying the amount of poly(ethylene glycol) and the exposure time of light to cure the ink. Freestanding tablets were produced, but only after the formulations had been dispensed into a preformed tablet and then removed (Acosta-Vélez et al., 2018).

Thin films for oral mucosal delivery have also been printed, using similar jet dispensing technologies. Ethanol based solutions with three bitter-tasting APIs (cetirizine HCl, diphenylhydramine HCl and ibuprofen) were formulated with eudragit (Scoutaris et al., 2015). Films were measured with the use of a calliper and were seen to be accurate, reproducible and uniform. The drugs existed in an amorphous state in the polymer matrix. This resulted in a fairly rapid drug release from the printed formulations. *In vivo* taste masking tests were done with human volunteers. The films did not rapidly disintegrate in the mouth (due to the polymer) and no bitterness was reported by the volunteers (Scoutaris et al., 2015).

In this paper, a model water-soluble drug, thiamine HCl, was selected. Thiamine HCl was selected due to its ease of availably, high water solubility, and low cost. As with the conventional tablet manufacturing process, the phase transformation of the drug is a possibility. Changes in drug phases can result in negative properties such as toxicity and bioavailability (Zhang et al., 2004). Commonly referred to as vitamin B1, the drug can exist as several polymorphic phases, including a non-stoichiometric hydrate (NSH), a hemihydrate (HH) and an anhydrate (AH). When exposed to methanol, thiamine HCl can also form a monomethanolate (MM) and a desolvated MM (Chakravarty and Suryanarayanan, 2010). In this investigation the two possible hydration states of thiamine HCl are the NSH and HH phase. The NSH is the starting material for manufacturing and the preferred state for tablets (Chakravarty et al., 2009). NSH can readily transform to the HH state when in contact with water, often in high humidity environments. The phase change begins with moisture adsorption on the NSH crystal surface. This causes some of the NSH crystals to dissolve or deliquesce. Recrystallisation of the HH crystals then occur as they have a lower water solubility (Masuda et al., 2011). Even though the HH is exceptionally stable, it

6

has lower aqueous solubility (Chakravarty et al., 2010) and has poorer powder flow characteristics (Masuda et al., 2011).

The aim of this investigation was to illustrate the ability to wholly inkjet print a free-standing tablet in a water-based formulation with solvent evaporation as the lone solidification mechanism. There is a common reluctance to use solvent inkjet printing as often toxic solvents may be required to formulate a printable ink, necessitating an additional processing step to ensure all residual solvent is removed during the manufacturing process. We show that it is possible to a use a non-toxic, water-based method of formulating a printable ink. The concern for uncured materials and high temperatures were therefore avoided with this method.

2 MATERIALS AND METHODS

2.1 MATERIALS

Polyvinylpyrrolidone (Mw ~ 10,000) (PVP), thiamine HCl (reagent grade, > 99%), polysorbate 20 (TWEEN20) and glycerol were used with deionised water to form the required ink formulation. All chemicals were purchased from Sigma Aldrich.

2.2 INK PREPARATION

The ink solutions were prepared by weighing components (PVP, thiamine HCl, polysorbate 20, glycerol and water) while being placed in glass vials. Solutions were heated (60 °C) and stirred (with a magnetic stirrer) until all components had been dissolved.

7

2.3 SURFACE TENSION AND CONTACT ANGLE MEASUREMENT

A Krüss Drop Shape Analyser (DSA100) was used for surface tension and contact angle measurements. For surface tension measurements, 1 mL of the ink was syringed and loaded onto the DSA. Small volumes of the ink were dosed through the syringe and an attached needle until a stable droplet had formed. Just before the droplet was dispensed, a profile of the droplet was taken from which surface tension is computationally calculated. To measure the ink's contact angle (θ), the substrate was raised to collect a drop from the syringe, minimising the effect of impact. The contact angle measurement was taken as soon the drop separated from the needle. Work of adhesion (W_A) values were calculated using the Young-Dupre Equation (Equation 2) with the contact angle and ink's surface tension values (Schrader, 1995). Measurements were taken at the ambient room temperature, which at the time was 23 °C.

$$W_A = \gamma(1 + \cos\theta) \quad (2)$$

2.4 VISCOSITY

Shear viscosity was measured using a Malvern Instruments Kinexus Pro Research Rheometer. A cup and bob set up was used to prevent solvent evaporation during the process. 3.09 mL of ink was syringed into the lower geometry (the cup) and the bob was automatically lowered into the cup. Shear viscosity was measured at shear rates between 1 s^{-1} and 1000 s^{-1}. The measurements at 100 s^{-1} were taken as a guide to the ink's viscosity during deposition. This is a widely accepted practice for determining the viscosity of Newtonian inks for jetting. In reality, shear rates during the jetting process can reach $10^5 - 10^6$ s^{-1} (Hoath, 2016). The temperature was fixed to 28 °C.

2.5 DENSITY

0.5 mL of the ink was syringed into a vial on a mass balance. The ratio between mass and volume was used to calculate the density of the ink.

8

2.6 DESIGN OF TABLET

Two dimensional (2D) bitmap files were created using Fujifilm Dimatix pattern editor software. A total of five rectangle-based patterns were printed to illustrate dose control with a single formulation (see Table S.1 in the ESI file for additional details).

2.7 PRINTING

Printing was conducted using a Fujifilm Dimatix Materials Printer DMP-2850 Series. 3 mL of ink was loaded into a cartridge through a 0.45 μm filter (preventing any large particles from blocking the 21 μm nozzles (Fujifilm, 2013)). A print head (10 pL) with 16 nozzles was then attached to the printer cartridge. The parameters for jetting that can be controlled were the jetting voltage, waveform, frequency and cartridge heating. Jetting behaviour can be observed by using the system's drop watcher feature. For print formation, parameters such as drop spacing, substrate heating and distance between the print head and substrate could be varied. As the ink formulation was water-based, the evaporation of water in the printing environment was the drying and solidification mechanism.

2.8 PRINT FORMATION CHARACTERISATION

A Nikon Eclipse LV100ND Optical Microscope was used to analyse the printed materials.

2.9 DETERMINING DRUG THEORETICAL DOSE

Using the Dimatix pattern editor software, the number of drops per layer for each pattern was calculated. With a known number of printed layers, the total number of droplets for each tablet was calculated.

Using the printer's drop watcher feature and ImageJ software, it was possible to measure the diameter of the individual droplets. The diameter of the nozzle of the cartridge was known and used for converting the pixel units to a unit of length.

9

The droplet diameter allowed the calculation of the volume. After density measurement of the ink, it was possible to calculate the mass of each droplet and with the composition of the ink known, the dose of thiamine HCl was calculated.

2.10 VALIDATION OF DRUG CONTENT

Elemental analysis by combustion was conducted with a LECO 628 Series Carbon/Hydrogen/Nitrogen determinator with a sulphur add-on module. The furnace was set at 1350 °C with oxygen at 40 PSI.

2.11 POLYMORPH IDENTIFICATION

A ThermoElectron FT-Raman NXR 9650 spectrometer was used to investigate the phase of thiamine HCl. Spectra were acquired using a 1064 nm laser (at a power of 0.6 mW) over the range 100-3701 cm^{-1}. The spectral resolution in this configuration was 4 cm^{-1}. 128 accumulations were used for each measurement. The laser spot size was 50 μm.

2.12 DRUG DISTRIBUTION INVESTIGATION

A Horiba Jobin Yvon LabRAM HR confocal Raman microscope with an automated xyz stage (Märzhäuser) was used to probe the distribution of the respective components within the tablet. Spectra were acquired using a 785 nm laser (at a power of 24 mW), a 100 x objective lens and a 300 μm confocal pinhole. To simultaneously scan a range of Raman shifts, a 600 lines mm^{-1} rotatable diffraction grating along a path length of 800 mm was employed. Spectra were acquired using a Synapse CCD detector (1024 pixels) thermoelectrically cooled to −60 °C. Before spectra collection, the instrument was calibrated using the zero-order line and a standard Si(100) reference band at 520.7 cm^{-1}. The spectral resolution in this configuration was <0.8 cm^{-1}.

10

Single point measurements of the individual components were acquired over the range 50-4000 cm^{-1}, with an acquisition time of 15 seconds and 4 accumulations to automatically remove the noise spikes due to cosmic rays and improve the signal to noise ratio.

Lateral spectroscopic maps of the top and bottom surfaces were obtained by collecting individual Raman spectra over the range $460 – 1760$ cm^{-1} in 10 μm steps from within a square 230 x 230 μm (a total of 576 spectra). Each spectrum was collected for 20 seconds, repeated once, thus each map required approximately 16 hours of acquisition time. The DuoScan functionality was employed to confer a spatial resolution of ~10 μm in all dimensions. An analogous spectroscopic line map of the cross section was obtained in 1 μm steps (a total of 968 spectra) using the AutoFocus function to correct for the uneven surface topography. The spatial location of the individual components of the formulation were evaluated within the respective data sets using Classic Least Squares (CLS) regression analysis within Labspec 6.4.3 software.

2.13 DRUG RELEASE STUDIES

A Copley dissolution tester (DIS 8000) was used for dissolution studies. For thiamine HCl, 500 mL volume of deionised water was used (specified in U.S Pharmacopeia (USP) (U.S. Pharmacopeia, 2018)). Media were heated to 37 °C using a water bath and paddles used for stirring (50 rpm). Samples were placed in media and at pre-determined time intervals a 1.5 mL aliquot was extracted and replaced by fresh solution. The extracted aliquots were filtered (0.45 μm) and then analysed with UV-Vis spectrophotometry (Varian Cary 50 UV-Vis Spectrophotometer). Solutions were syringed into a quartz cuvette and scanned. The absorbance at 266 nm was used to quantify the drug amount.

Calibration standards were also prepared by dissolving thiamine HCl in deionised water and preparing serial dilutions. Standard solutions were analysed using UV-Vis spectrophotometry and a calibration line was plotted based on the absorbance detected at 266 nm. The intensity of the diagnostic

11

peak for thiamine HCl at 266 nm was used to calculate the amount of drug released through the application of the Beer-Lambert law.

3   RESULTS AND DISCUSSION

3.1   INK DEVELOPMENT

With the two main components of the formulation (PVP and thiamine HCl) being water soluble, water could be readily used as the solvent. As water has a high surface tension, the surfactant polysorbate 20 was added to the formulation to reduce the surface tension of the ink to 37.05 mNm^{-1} (originally measured at 65.55 mNm^{-1}) and hence improve printability. Furthermore, glycerol was added as a plasticiser to avoid cracking during drying and to allow easy handling of the tablet. Without the addition of the plasticiser, the printed tablets were brittle and susceptible to fracture during both the printing process and subsequent substrate removal. The final ink composition consisted of PVP (14 wt%), thiamine HCl (10 wt%), polysorbate 20 (1 wt%), glycerol (1 wt%) and deionised water (74 wt%). Table 1 displays the ink's surface tension, viscosity, density, the printer's nozzles diameter. The Z value of the ink was calculated to be 5.0, which is well within the printable range. Additional rheological data can be found in Figure S.1 in the ESI file.

3.2   SELECTION OF PRINTING PARAMETERS

3.2.1   Jetting of ink

Standard jetting parameters were used for printing the ink. This included a jetting voltage and frequency of 16 V and 5 kHz respectively. A waveform for model fluids (see Figure S.2 in ESI file) for the printer was also used. The cartridge and substrate temperature were kept at 28 °C, to illustrate the

12

ability to print drug containing formulations at lower temperatures. The resultant jetting had stable and reliable droplet formation (see Figure S.3 in ESI file).

3.2.2 Substrate selection

The choice of substrate was an important manufacturing decision. An ink must adhere well to the substrate during the printing process as well as being easily removable once printing is completed. A 5x5 mm square was printed (100 layers) on both glass slides and polyethylene terephthalate (PET) films. The tablets on glass were extremely difficult to remove and often resulted in the fracture of the tablet form. Conversely, the removal of tablets from the PET film were possible with no observable damage. This was achieved by bending the PET film causing the tablets to 'pop off'. This difference in behaviour was attributed to the contact angle and in turn its work of adhesion of the ink on the substrates. On the glass slide, the contact angle and work of adhesion was 29.1 ± 2.6 ° and 69.4 ± 0.8 mN·m^{-1} (n = 5) respectively. On PET film contact angle increased to 53.4 ± 1.8 ° and work of adhesion decreased to 59.1 ± 0.9 mN·m^{-1} (n = 5). A smaller contact angle (caused by more ink spreading and in turn a larger work of adhesion) meant more force was required to remove the ink from the substrate.

3.2.3 Printing parameters

Substrate temperature was maintained at 28 °C. Initially, individual droplets were jetted on the PET substrate. As Figure 1 shows, the printed drops were well-defined with a mean diameter of 30 ± 2 μm (n = 9). Common problems associated with solvent inkjet printing such as the coffee-ring effect and build-up of solid material on edges on of the drop were not observed.

Following this, line and film formation were investigated with different drop spacings. As noted in Figure 2, using a 40 μm drop spacing it was not possible to form both uniform lines and films - as the distance between droplets was significantly larger than their diameter. With 20 and 30 μm drop spacings, complete lines were formed, but some bulging was observed, more so with 20 μm drop spacing. The film

13

formation for 20 µm drop spacing showed a complete film with no gaps, in contrast to the 30 µm drop spacing film, which exhibited patchier coverage. It was decided to use the 20 µm drop spacing for the printing of tablets based on this ability to produce a uniform two-dimensional film.

Two occurrences of phase separation in the printed films were observed during the printing and drying process. The first process could be seen as time progresses after the printed films have dried. This process was seen as crystal growth, which we attribute to thiamine HCl, being the only crystalline component in the formulation. Figure 3 shows a single layer of the formulation printed on a glass slide. The optical images in reflection clearly show that crystals nucleate with time, ultimately forming a suspension of thiamine HCl crystals in PVP, confirmed in the cross-polarised images in transmission.

The second occurrence of phase separation was observed as additional layers were printed. Initially, films were uniformly clear, but as more material was added white grains were seen to form, shown in Figure 4. As more layers were printed, the white grains grew, eventually leading to a uniformly white tablet, as seen in Figure 5. The most likely explanation for this is a solvent mediated recrystallisation process (Cardew and Davey, 1985). The addition of a solvent (in this case, water from the ink), dissolves the previously printed drug, increasing the total concentration of drug available in the liquid phase, resulting in the nucleation and growth of larger crystals.

The time to manufacture printed tablets was heavily controlled by the evaporation time of water and the number of tablets being printed. When a single row of ten tablets (5 x 5 mm square design) was printed (one minute was required for one layer to be printed), it was determined at least one minute was required for complete evaporation of water (based on visual observations). Any less time resulted in spreading of ink and loss of shape of the tablets. An inter-layer delay of one minute was hence required when printing tablets. When producing ten tablets with a 5 mg dose (250 layers) (see Table S.1 in ESI file) it would take 500 minutes including the delay. In contrast to more conventional manufacturing methods of tablets, where an output of 500,000 tablets per hour can be achieved (Gerhardt, 2010), the

14

inkjet process used here is very slow. Inkjet printing would therefore seem to be more suited to produce personalised, patient-specific tablets where such large outputs are not required. It should be noted that printers do exist where a greater number of nozzles are available for use, illustrating potential for scaling up and speeding up the inkjet process.. For example, Kyobula et al., 2017 used a PIXDRO LP-50 printer where 128 nozzles were available (Kyobula et al., 2017). A proof-of-concept continuous printing system has also been developed for the inkjet printing of orodispersible films using PIXDRO JS 20 jetting station (128 nozzles) (Thabet et al., 2018).

The optimisation of inkjet printing for tablet manufacturing would be very advantageous to investigate. This would include ways of optimising the large print times as well as making efficient use of the space available on the print bed. For example, printing a row of tablets with an inter-layer delay would be less efficient than printing two rows of tablets, which would allow for a greater number of samples produced with the same time. The speed of tablet manufacturing with inkjet printing can be controlled by a range of printing settings including jetting frequency, number of nozzles used, drop spacing, size of the pattern, orientation of pattern, spacing between patterns and number of pattern repeats (x and y direction on the print bed). Substrate heating could also influence printing time by changing the rate at which solvent would evaporate. In addition to this, a wide array of different designs can be printed at the same time highlighting inkjet printing as a method of producing tablets with different doses in a single printing process. Increasing the number of printers used in the manufacturing process could potentially increase output and speed of printing tablets.

3.3 DRUG CONTENT INVESTIGATION

As thiamine HCl is the only sulphur containing component of the formulation, this element was used to quantify the content of thiamine HCl in the tablets (based on mass %). The mean sulphur content from thiamine HCl powder and a printed tablet was, 10.11 ± 0.10 % and 4.03 ± 0.06 % (n = 3) respectively.

15

Using the values measured, it was determined that the thiamine HCl content in the tablet was 39.8% (i.e. 4.03 / 10.11). This value is close to the expected value of 38.4% thiamine HCl content calculated from the composition of the solid components of the formulation of the ink and thus the jetted material corresponded reliably to the formulated ink composition.

3.4 POLYMORPH INVESTIGATION

Raman spectroscopy was definitive in identifying the phase of thiamine HCl. For NSH, a single peak associated with a C=C stretching vibration from the aromatic group of the drug is seen at 1607 cm^{-1} (Mazurek and Szostak, 2012), whereas for HH, two closely spaced peaks at 1594 and 1614 cm^{-1} are observed. An additional peak at 1332 cm^{-1} is also noted in the Raman spectrum of the HH form (Mazurek and Szostak, 2012). As can be clearly seen from Figure 6, the tablet – like the parent powder – was found to exist in the NSH polymorphic phase based on the spectra collected from random points on both its the top and bottom faces. Similarly, the Raman spectra of a single tablet placed overnight in a vacuum oven to remove all moisture, broken and subsequently ground to a powder, was also consistent with the NSH phase, suggesting that the NSH phase of thiamine HCl is ubiquitous within the bulk tablet. Thiamine HCl tablets produced by conventional means are known to undergo a phase change over time (Chakravarty et al., 2012). Therefore, to confirm the time-dependent stability of thiamine HCl in both the tablet and parent ink, analysis of (i) tablets printed and kept in an ambient environment for two months and (ii) tablets printed with an ink kept in an ambient environment for one month was conducted, respectively. Critically, no differences in the Raman spectra were observed relative to those obtained from fresh formulations, suggesting that thiamine HCl remains in the NSH phase in a stable manner at least over these time frames. Thiamine HCl powder that was exposed to the ambient environment for a prolonged time did undergo a phase change to the HH phase (as expected) with the peak at 1332 cm^{-1} clearly forming, as well as peaks at 1594 and 1614 cm^{-1}, shown in Figure 6.

16

3.5 DRUG SPATIAL DISTRIBUTION

To probe the distribution of thiamine HCl, PVP, polysorbate 20 and glycerol within the printed formulation, the top and bottom surfaces were analysed by confocal Raman microscopy (Figure 7; S.6 and S.7 in the ESI file). For each surface, the homogeneity of thiamine HCl incorporation was the corresponding false colour images constructed using classic least squares (CLS) regression analysis. In this intuitive approach, each spectrum of the dataset is expressed as the linear combination of the pure component spectra, with the resultant scores calculated via least square regression in such a way that the residuals are minimised, normalised and then plotted to generate the map. Importantly, both top and bottom surface maps show a relatively uniform distribution of thiamine HCl within the appraised areas, with subtle variation in the top surface map associated with a greater extent of surface roughness. However, the high homogeneity of thiamine HCl loading observed for both surfaces were exemplified by near-identical mean values and low standard deviation of thiamine HCl CLS scores obtained from the maps: 55.5 ± 6.1 % (11 %, N= 576) and 55.3 ± 4.3 % (8 %, N = 576) from the top and bottom surfaces, respectively. To further explore the distribution of thiamine HCl within the tablet, the tablet was cut with a scalpel and the cross-section analysed by Raman spectroscopic mapping (Figure S.8 in the ESI file). A mean thiamine HCl CLS score of 54.5 ± 10.8 % (20 %, N = 968) was obtained, providing further evidence for the homogeneous distribution of the drug within the total formulation. No peaks indicative of the HH phase were observed in any of the map spectra (Figure 8), supporting the data obtained from single point measurements from the bulk samples (Figure 6).

3.6 DRUG RELEASE BEHAVIOUR

The theoretical dose of tablets was calculated using the number of drops jetted per layer and per tablet (see Table S.1 in ESI). Using this data and ImageJ data where the in-flight droplet diameter was calculated to be 22 ± 1 μm (n = 4), the theoretical dose for each tablet was determined.

17

From Figures 9 and 10, all batches of tablets showed a rapid drug release with all reaching 90% within 7 minutes. On varying the number of printed layers, no clear trend can be seen with respect to the time required for complete dissolution highlighting the rapid dissolution of the formulation. With samples that have varied pattern dimensions, a subtle trend can be seen possibly due to differences in the amount of material required to print these samples being greater. However, the error bars (standard deviation associated with repeat measurements) are large and thus definitive conclusions cannot be drawn, except that the amount of drug released varied rapidly compared to the time-frame of the measurements taken.

There is a small apparent discrepancy between the theoretical and measured dose for tested samples ($\pm 5 - 10$ %). However, the USP for thiamine HCl tablets allows drug release to be between $90 - 110$ % of the theoretical dose, hence all results reported here are acceptable (U.S. Pharmacopeia, 2018). The differences between the theoretical and measured dose could be caused by a number of reasons. These include errors made in the printing process (e.g. blocked nozzles), incorrect assumptions associated with the printing process (e.g. all droplets are spherical) or due to the lack of accuracy of the drop watcher camera. There is however good correlation between the measured doses and the sample details (e.g. halving the pattern size or number of layers leads to halving of the dose, see Table S.1 in ESI file), suggesting good consistency of the printing process.

4   CONCLUSIONS

Solvent inkjet printing has been used to 3D print free-standing tablets from a water based formulation. Using water-soluble PVP based-ink and thiamine HCl as a model API, a printable ink was developed using polysorbate 20 and glycerol as additives. Appropriate surface tension and viscosity values were measured and optimum print parameters were investigated. Through the initial printing of up to 10 layers, it was observed that two phase separation processes occur: one as a function of time and the other related to the number of layers printed. Optical microscopy imaging show the thiamine HCl crystals

18

exist as a suspension in PVP. Combustion analysis confirmed the successful translation of the composition of the ink into the printed tablet, which contained thiamine HCl in the ideal NSH polymorphic form distributed uniformly throughout the formulation. Given the high solubility of the API and polymer excipient, drug release was rapid to such an extent that it was not possible to control it by varying the 2D pattern and number of layers. However, this process used no toxic materials, did not need extreme conditions (e.g. high temperatures), nor used secondary printing methods to produce a wholly inkjet printed tablet, without incorporating an edible substrate that would require cutting and encapsulation. The ink formulated in this investigation can potentially be used as a 'universal' pharmaceutical formulation for any water soluble API. Investigation of the tablet's mechanical properties (such as hardness and friability) should be conducted to better characterise the handling and physical integrity of the tablets.

ACKNOWLEDGEMENTS

APPENDIX A. SUPPLEMENTARY DATA

Supplementary data to this article can be found online.

REFERENCES

Acosta-Vélez, G.F., Linsley, C.S., Craig, M.C., Wu, B.M., 2017. Photocurable Bioink for the Inkjet 3D Pharming of Hydrophilic Drugs. Bioengineering 4, 1–11. https://doi.org/10.3390/bioengineering4010011

19

Acosta-Vélez, G.F., Zhu, T.Z., Linsley, C.S., Wu, B.M., 2018. Photocurable Poly(ethylene glycol) as a Bioink for the Inkjet 3D Pharming of Hydrophobic Drugs. Int. J. Pharm. Accepted M. https://doi.org/10.1016/j.quageo.2010.03.003

ASTM International, 2013. F2792-12a - Standard Terminology for Additive Manufacturing Technologies. Rapid Manuf. Assoc. https://doi.org/10.1520/F2792-12A.2

Baumers, M., Wildman, R., Wallace, M., Yoo, J., Blackwell, B., Farr, P., Roberts, C.J., 2018. Using total specific cost indices to compare the cost performance of additive manufacturing for the medical devices domain. Proc. Inst. Mech. Eng. Part B J. Eng. Manuf. 1–15. https://doi.org/10.1177/0954405418774591

Cardew, B.T., Davey, R.J., 1985. The kinetics of solvent-mediated phase transformations 398, 415–428.

Chakravarty, P., Berendt, R.T., Munson, E.J., Young JR., V.G., Govindarajan, R., Suryanarayanan, R., 2009. Insights into the Dehydration Behavior of Thiamine Hydrochloride (Vitamin B1) Hydrates: Part I. J. Pharm. Sci. 99, 816–827. https://doi.org/10.1002/jps

Chakravarty, P., Govindarajan, R., Suryanarayanan, R.A.J., 2010. Investigation of Solution and Vapor Phase Mediated Phase Transformation in Thiamine Hydrochloride. J. Pharm. Sci. 99, 3941–3952. https://doi.org/10.1002/jps

Chakravarty, P., Suryanarayanan, R., 2010. Characterization and Structure Analysis of Thiamine Hydrochloride Methanol Solvate. Cryst. Growth Des. 10, 4414–4420. https://doi.org/10.1021/cg100522f

Chakravarty, P., Suryanarayanan, R., Govindarajan, R., 2012. Phase Transformation in Thiamine Hydrochloride Tablets: Influence on Tablet Microstructure Physical Properties and Performance. J. Pharm. Sci. 101, 1410–1422. https://doi.org/10.1002/jps

Cheow, W.S., Kiew, T.Y., Hadinoto, K., 2015. Combining inkjet printing and amorphous nanonization to prepare personalized dosage forms of poorly-soluble drugs. Eur. J. Pharm. Biopharm. 96, 314–321. https://doi.org/10.1016/j.ejpb.2015.08.012

20

Clark, E.A., Alexander, M.R., Irvine, D.J., Roberts, C.J., Wallace, M.J., Sharpe, S., Yoo, J., Hague, R.J.M., Tuck, C.J., Wildman, R.D., 2017. 3D printing of tablets using inkjet with UV photoinitiation. Int. J. Pharm. 529, 523–530. https://doi.org/10.1016/j.ijpharm.2017.06.085

Cummins, G., Desmulliez, M.P.Y., 2012. Inkjet printing of conductive materials: a review. Circuit World 38, 193–213. https://doi.org/10.1108/03056121211280413

Derby, B., 2010. Inkjet Printing of Functional and Structural Materials: Fluid Property Requirements, Feature Stability, and Resolution. Annu. Rev. Mater. Res. 40, 395–414. https://doi.org/10.1146/annurev-matsci-070909-104502

Desai, S., Perkins, J., Harrison, B.S., Sankar, J., 2010. Understanding release kinetics of biopolymer drug delivery microcapsules for biomedical applications. Mater. Sci. Eng. B Solid-State Mater. Adv. Technol. 168, 127–131. https://doi.org/10.1016/j.mseb.2009.11.006

Edinger, M., Bar-Shalom, D., Rantanen, J., Genina, N., 2017. Visualization and Non-Destructive Quantification of Inkjet-Printed Pharmaceuticals on Different Substrates Using Raman Spectroscopy and Raman Chemical Imaging. Pharm. Res. 1023–1036. https://doi.org/10.1007/s11095-017-2126-2

Edinger, M., Bar-Shalom, D., Sandler, N., Rantanen, J., Genina, N., 2018. QR encoded smart oral dosage forms by inkjet printing. Int. J. Pharm. 536, 138–145. https://doi.org/10.1016/j.ijpharm.2017.11.052

Fina, F., Madla, C.M., Goyanes, A., Zhang, J., Gaisford, S., Basit, A.W., 2018. Fabricating 3D printed orally disintegrating printlets using selective laser sintering. Int. J. Pharm. 541, 101–107. https://doi.org/10.1016/j.ijpharm.2018.02.015

Fox, C.B., Nemeth, C.L., Chevalier, R.W., Cantlon, J., Bogdanoff, D.B., Hsiao, J.C., Desai, T.A., 2017. Picoliter-volume inkjet printing into planar microdevice reservoirs for low-waste, high-capacity drug loading. Bioeng. Transl. Med. 9–16. https://doi.org/10.1002/btm2.10053

Fujifilm, 2013. Jettable Fluid Formulation Guidelines, Fujifilm Support Documentation.

Genina, N., Fors, D., Palo, M., Peltonen, J., Sandler, N., 2013. Behavior of printable formulations of loperamide and caffeine on different substrates - Effect of print density in inkjet printing. Int. J.

Pharm. 453, 488–497. https://doi.org/10.1016/j.ijpharm.2013.06.003

Genina, N., Fors, D., Vakili, H., Ihalainen, P., Pohjala, L., Ehlers, H., Kassamakov, I., Haeggström, E., Vuorela, P., Peltonen, J., Sandler, N., 2012. Tailoring controlled-release oral dosage forms by combining inkjet and flexographic printing techniques. Eur. J. Pharm. Sci. 47, 615–623. https://doi.org/10.1016/j.ejps.2012.07.020

Gerhardt, A.H., 2010. Fundamentals of Tablet Compression. J. GXP compliance 14, 70–79.

Gibson, I., Rosen, D.W., Stucker, B., 2010. Additive Manufacturing Technologies. https://doi.org/10.1007/978-1-4419-1120-9

Gibson, M., 2009. Pharmaceutical Preformulation and Formulation, 2nd ed. https://doi.org/10.1021/op050157h

He, Y., Tuck, C.J., Prina, E., Kilsby, S., Christie, S.D.R., Edmondson, S., Hague, R.J.M., Rose, F.R.A.J., Wildman, R.D., 2017. A new photocrosslinkable polycaprolactone-based ink for three-dimensional inkjet printing. J. Biomed. Mater. Res. - Part B Appl. Biomater. 105, 1645–1657. https://doi.org/10.1002/jbm.b.33699

He, Y., Wildman, R.D., Tuck, C.J., Christie, S.D.R., Edmondson, S., 2016. An Investigation of the Behavior of Solvent based Polycaprolactone ink for Material Jetting. Sci. Rep. 6, 1–10. https://doi.org/10.1038/srep20852

Hirshfield, L., Giridhar, A., Taylor, L.S., Harris, M.T., Reklaitis, G. V., 2014. Dropwise additive manufacturing of pharmaceutical products for solvent-based dosage forms. J. Pharm. Sci. 103, 496–506. https://doi.org/10.1002/jps.23803

Hoath, S.D., 2016. Fundamentals of Inkjet Printing.

Khaled, S.A., Burley, J.C., Alexander, M.R., Yang, J., Roberts, C.J., 2015. 3D printing of five-in-one dose combination polypill with defined immediate and sustained release profiles. J. Control. Release 217, 308–314. https://doi.org/10.1016/j.jconrel.2015.09.028

Kyobula, M., Adedeji, A., Alexander, M.R., Saleh, E., Wildman, R., Ashcroft, I, Gellert, P.R., Roberts,

22

C.J., 2017. 3D inkjet printing of tablets exploiting bespoke complex geometries for controlled and tuneable drug release. J. Control. Release 261, 207–215. https://doi.org/10.1016/j.jconrel.2017.06.025

Magdassi, S., 2009. The Chemistry of Inkjet Inks.

Martin, G.D., Hoath, S.D., Hutchings, I.M., 2008. Inkjet printing - the physics of manipulating liquid jets and drops, in: Journal of Physics: Conference Series. p. 012001. https://doi.org/10.1088/1742-6596/105/1/012001

Masuda, K., Ishige, T., Yamada, H., Fujii, K., Uekusa, H., Miura, K., Yonemochi, E., Terada, K., 2011. Study of the Pseudo-Crystalline Transformation from Form I to Form II of Thiamine Hydrochloride (Vitamin B1). Chem. Pharm. Bull. (Tokyo). 59, 57–62. https://doi.org/10.1248/cpb.59.57

Mazurek, S., Szostak, R., 2012. Quantitative analysis of thiamine hydrochloride in tablets—Comparison of infrared attenuated total reflection, diffuse reflectance infrared and Raman spectroscopy. Vib. Spectrosc. 62, 10–16. https://doi.org/10.1016/j.vibspec.2012.07.006

Palo, M., Kogermann, K., Laidma, I., Meos, A., Preis, M., Heina, J., 2017. Development of Oromucosal Dosage Forms by Combining Electrospinning and Inkjet Printing. https://doi.org/10.1021/acs.molpharmaceut.6b01054

Pardeike, J., Strohmeier, D.M., Schrödl, N., Voura, C., Gruber, M., Khinast, J.G., Zimmer, A., 2011. Nanosuspensions as advanced printing ink for accurate dosing of poorly soluble drugs in personalized medicines. Int. J. Pharm. 420, 93–100. https://doi.org/10.1016/j.ijpharm.2011.08.033

Sandler, N., Maattanen, A., Ihalainen, P., Kronberg, L., Meierjohann, A., Viitala, T., Peltonen, J., 2011. Inkjet Printing of Drug Substances and Use of Porous Substrates-Towards Individualized Dosing. J. Pharm. Sci. Sci. 100, 3386–3395. https://doi.org/10.1002/jps

Schrader, M.E., 1995. Young-Dupre Revisited. Langmuir 11, 3585–3589. https://doi.org/10.1021/la00009a049

Scoutaris, N., Alexander, M.R., Gellert, P.R., Roberts, C.J., 2011. Inkjet printing as a novel medicine

23

formulation technique. J. Control. Release 156, 179–185. https://doi.org/10.1016/j.jconrel.2011.07.033

Scoutaris, N., Snowden, M., Douroumis, D., 2015. Taste masked thin films printed by jet dispensing. Int. J. Pharm. 494, 619–622. https://doi.org/10.1016/j.ijpharm.2015.05.018

Sturgess, C., Tuck, C.J., Ashcroft, I.A., Wildman, R.D., 2017. 3D reactive inkjet printing of polydimethylsiloxane. J. Mater. Chem. C 9733–9743. https://doi.org/10.1039/C7TC02412F

Thabet, Y., Sibanc, R., Breitkreutz, J., 2018. Printing pharmaceuticals by inkjet technology: Proof of concept for stand-alone and continuous in-line printing on orodispersible films. J. Manuf. Process. 35, 205–215. https://doi.org/10.1016/j.jmapro.2018.07.018

U.S. Pharmacopeia, 2018. Thiamine Hydrochloride Tablets [WWW Document]. URL http://www.pharmacopeia.cn/v29240/usp29nf24s0_m82500.html (accessed 4.16.18).

Vakili, H., Kolakovic, R., Genina, N., Sandler, N., 2014. Hyperspectral imaging in quality control of inkjet printed dosage forms. Int. J. Pharm. 483, 244–249.

Wang, J., Goyanes, A., Gaisford, S., Basit, A.W., 2016. Stereolithographic (SLA) 3D printing of oral modified-release dosage forms. Int. J. Pharm. 503, 207–212. https://doi.org/10.1016/j.ijpharm.2016.03.016

Wickström, H., Nyman, J.O., Indola, M., Sundelin, H., Kronberg, L., Preis, M., Rantanen, J., Sandler, N., 2016. Colorimetry as Quality Control Tool for Individual Inkjet-Printed Pediatric Formulations. AAPS PharmSciTech. https://doi.org/10.1208/s12249-016-0620-1

Wickström, H., Palo, M., Rijckaert, K., Kolakovic, R., Nyman, J.O., Määttänen, A., Ihalainen, P., Peltonen, J., Genina, N., Beer, T. De, Löbmann, K., Rades, T., Sandler, N., 2015. Improvement of dissolution rate of indomethacin by inkjet printing. Eur. J. Pharm. Sci. 75, 91–100. https://doi.org/10.1016/j.ejps.2015.03.009

Wu, B.M., Borland, S.W., Giordano, R.A., Cima, L.G., Sachs, E.M., Cima, M.J., 1996. Solid free-form fabrication of drug delivery devices. J. Control. Release 40, 77–87.

Zhang, G.G.Z., Law, D., Schmitt, E.A., Qiu, Y., 2004. Phase transformation considerations during process development and manufacture of solid oral dosage forms. Adv. Drug Deliv. Rev. 56, 371–390. https://doi.org/10.1016/j.addr.2003.10.009

Table 1 - Ink and printer properties for the rapid release formulation.

Figure 1 – 100 x optical microscope image of ink droplet printed on PET film (scale bar: 10 μm). Inset: 20 x magnification of drops on PET (scale bar: 100 μm).

Figure. 2 – Single line (top) and films (bottom) printed with one nozzle with varying drop spacing. Numbers indicate drop spacing. Scale bar = 500 μm.

Figure 3 – Optical reflection images of printed films on glass slide. a) 30 minutes after printing, b) 1 day, c) 4 days, d) 8 days, e) 12 days, f) 12 days after orienting confirm the formation of a crystalline phase (cross polarised transmission OM). Scale bar = 500 μm.

Figure 4 – Printed films with layers 8, 9 and 10 (top to bottom). Scale bar = 10 mm.

Figure 5 – Completed printed tablets. Scale bar = 1 cm

Figure 6 – Raman spectra of the thiamine HCl powder and different printed samples all showing peak positions indicative of the NSH phase. Also shown in the drug powder exposed to the ambient environment with features of the HH phase.

Figure 7 – Optical image (a) and CLS score map for thiamine HCl (b) from the top surface. Optical image (c) and CLS score map for thiamine HCl (d) from the bottom surface. It is important to note that as Raman spectra are known to be sensitive to nonlinearity, temperature effects and wavelength shifts, the determined scores from CLS fitting do not represent absolute component concentrations, i.e. are not expected to match those based on the composition of the ink. Thus the analysis is semi-quantitative, used to describe the relative contribution from the respective components as a function of spatial location.

Figure 8 – Mean spectra generated from the top and bottom surface lateral maps and the cross-section line measurement.
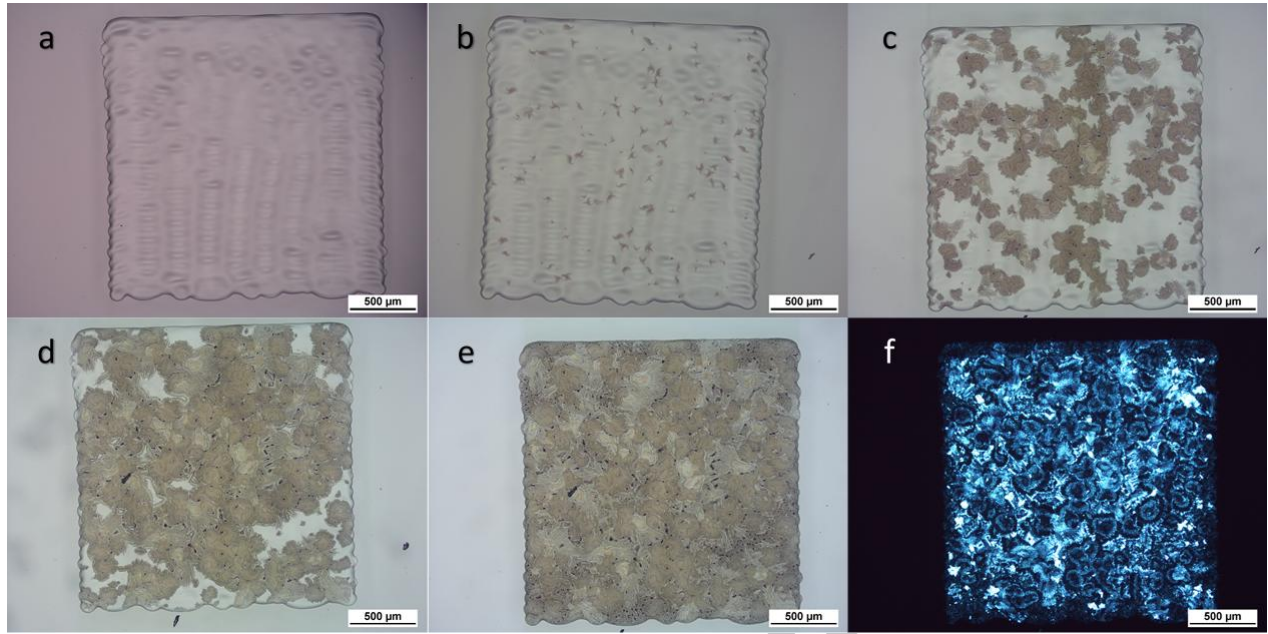
Figure 9 – Release profiles of tablets with varying printed layers. The printed pattern's dimensions were set at 5 x 5 mm (n=3 except for 375L where n=2).
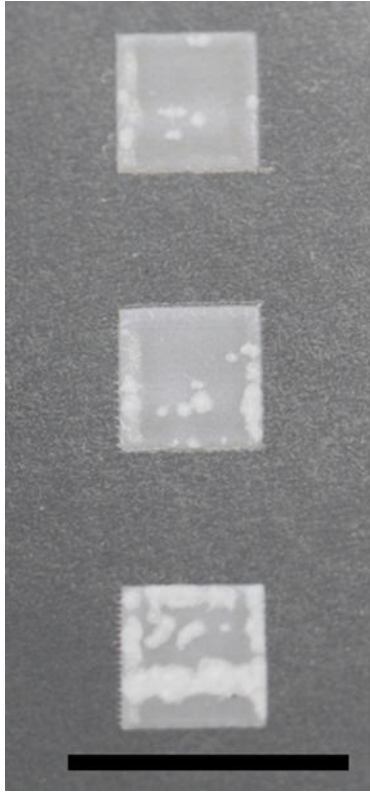
Figure 10 – Release profiles of tablets with varying pattern dimensions. The number of layers for each print were kept at 250 layers (n=3).
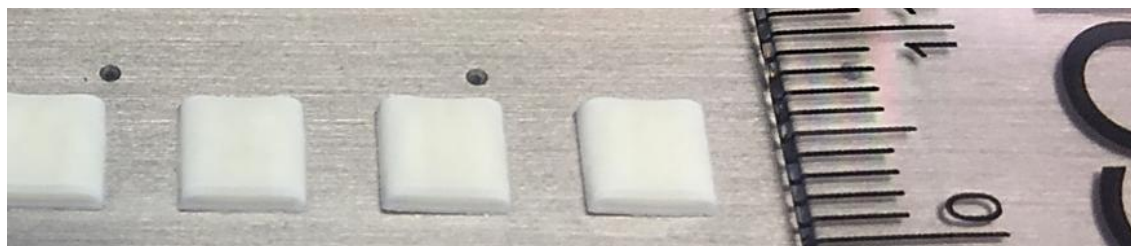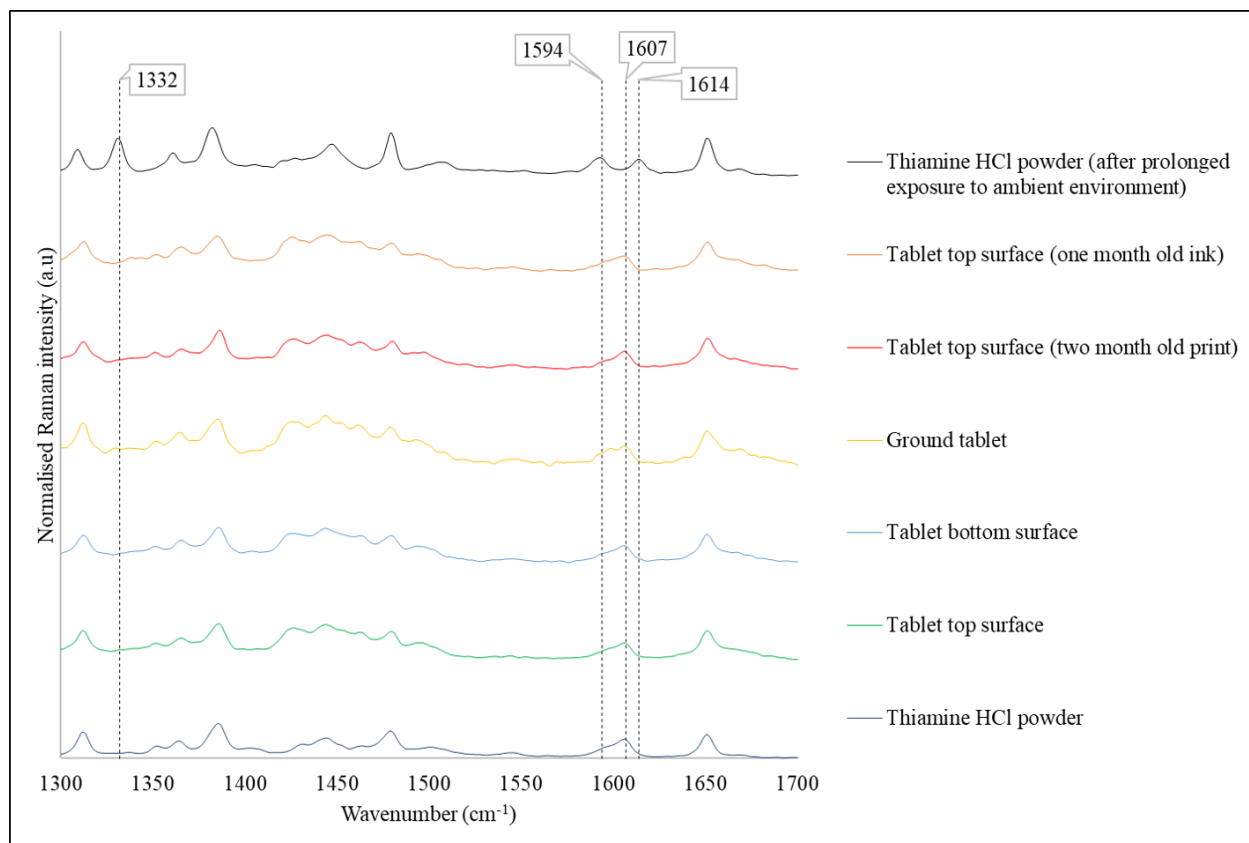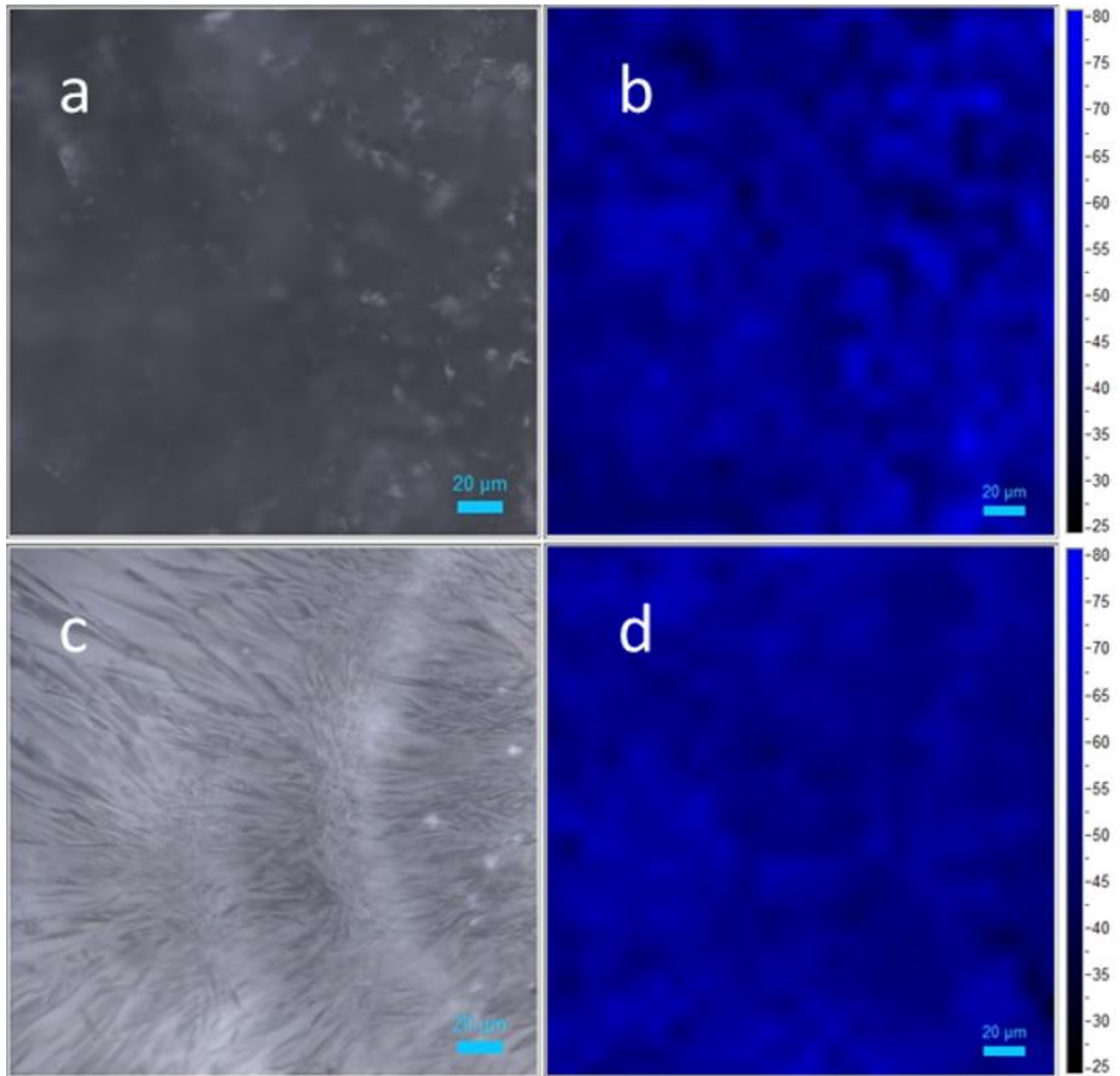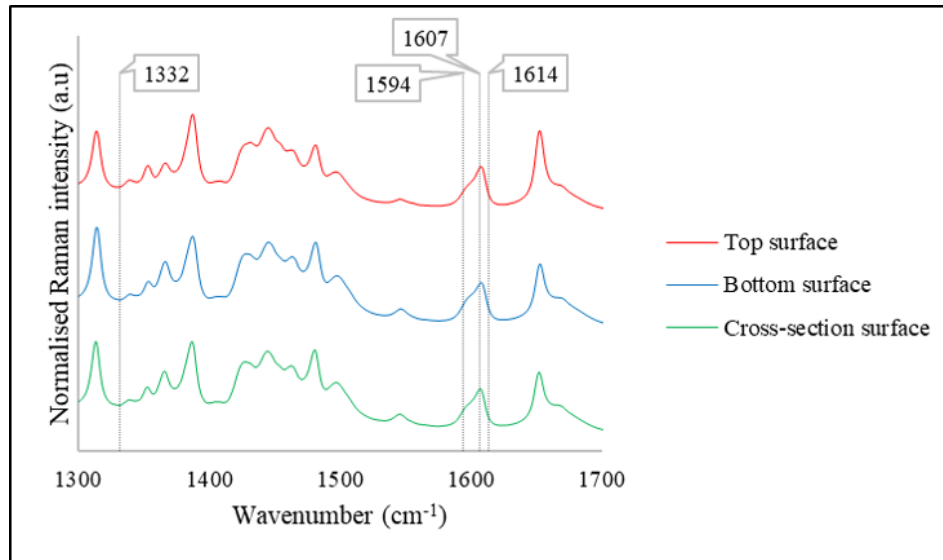
26

29

30

31

35

37
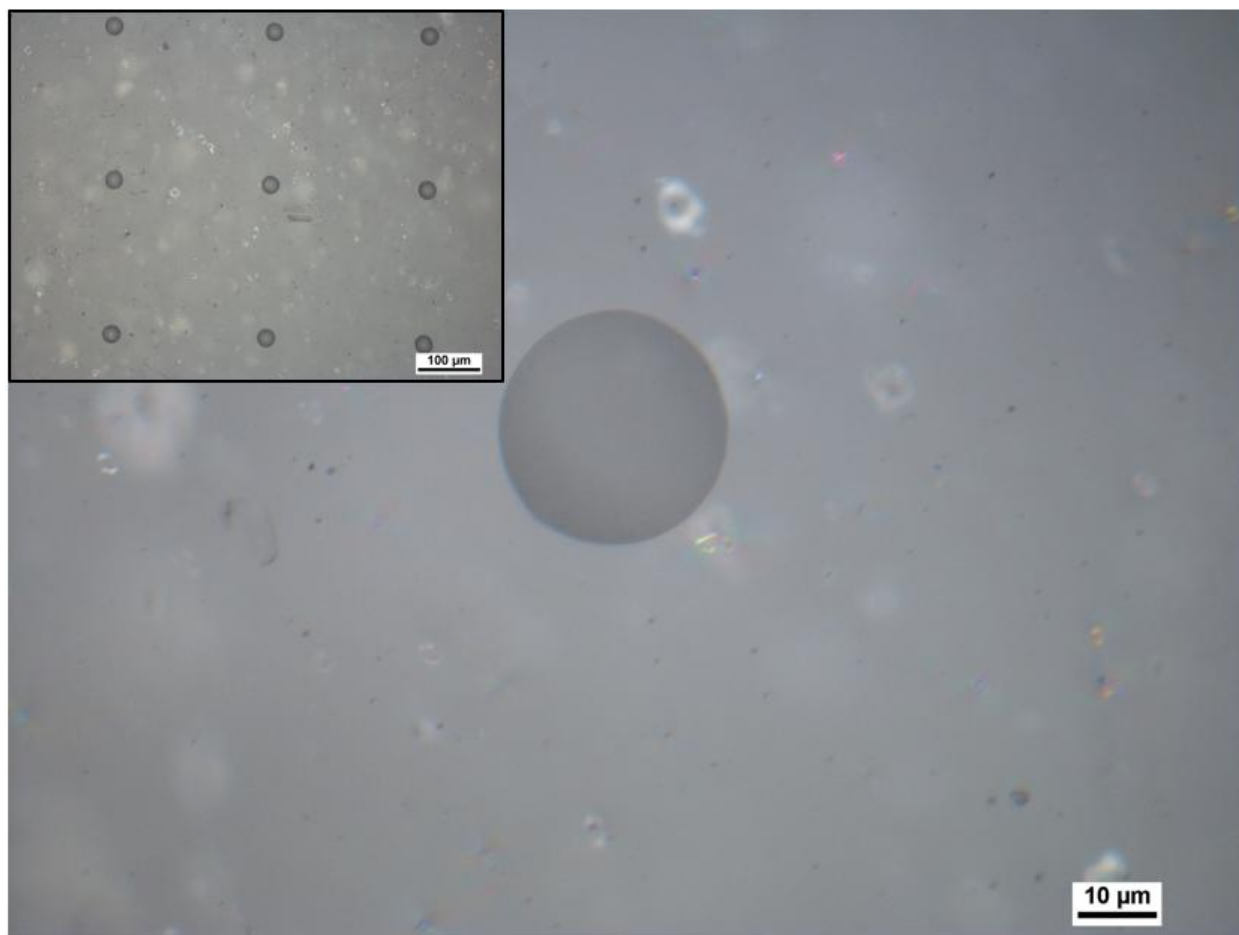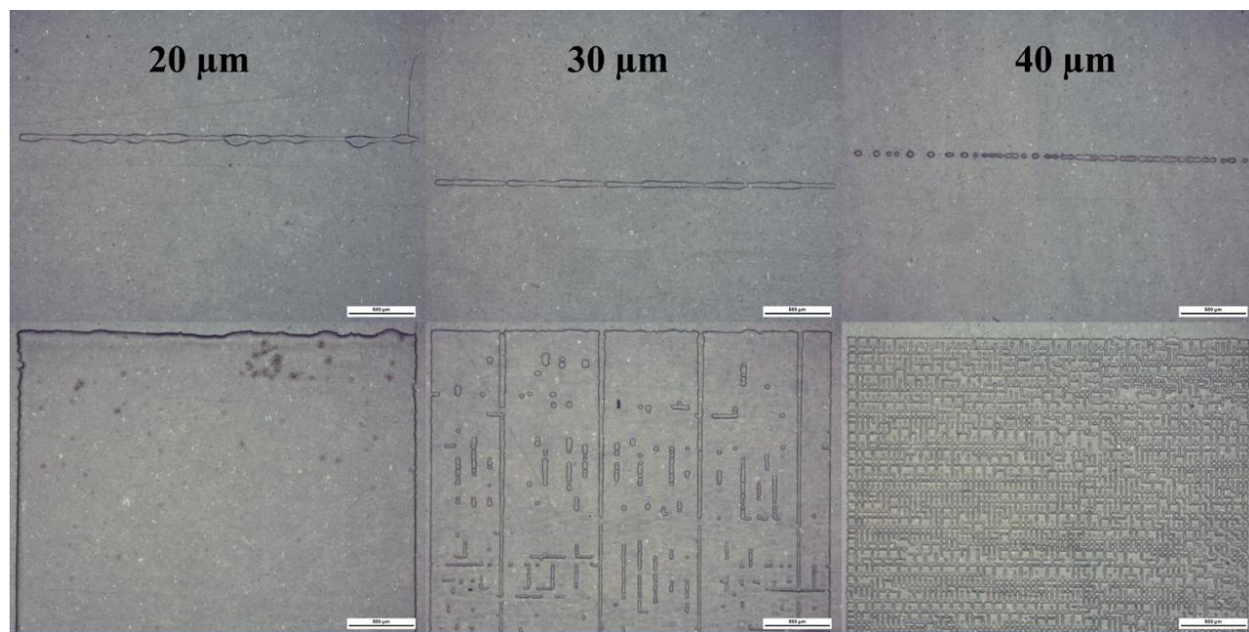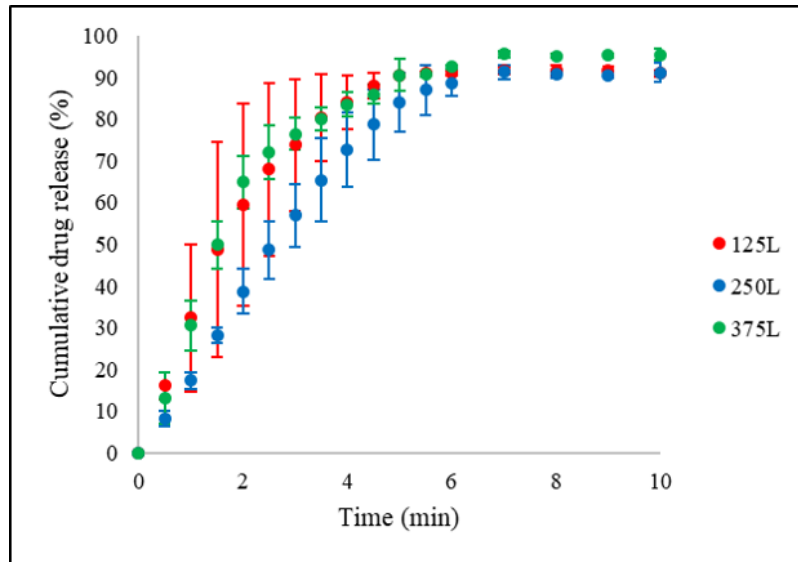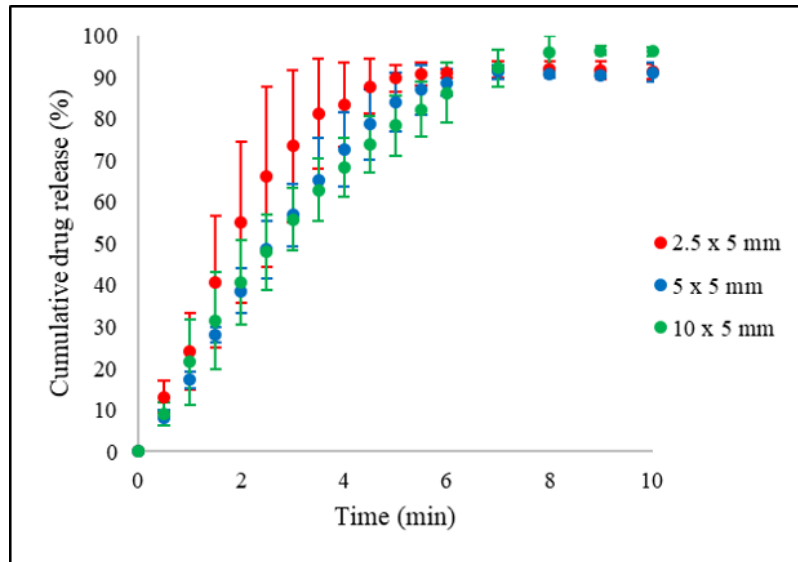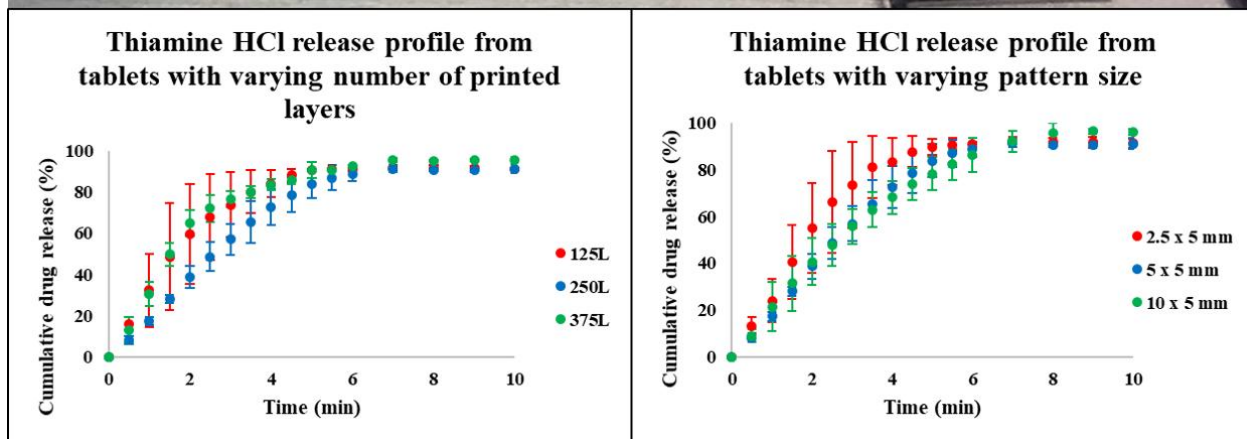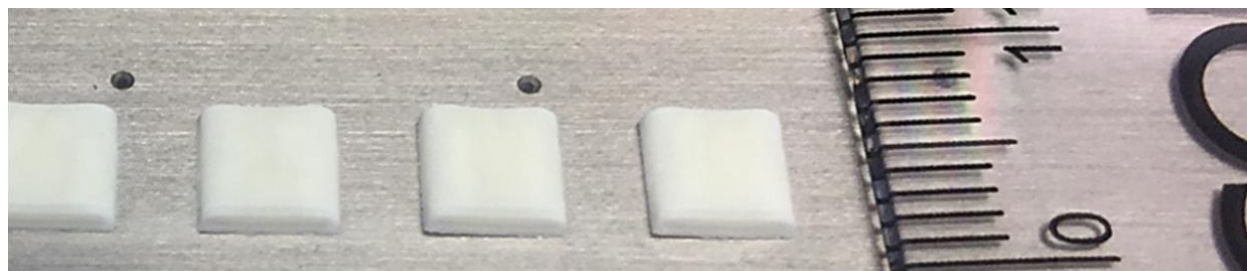
Surface tension (mN·m^{-1})	37.05 ± 0.67
Viscosity (mPa·s)	6.100 ± 0.074
Density (gmL^{-1})	1.2 ± 0.001
Nozzle diameter (µm)	21
Z factor	5.0